CHARACTERIZATION OF KNEE IMPACTS IN FRONTAL CRASHES

Jonathan D. Rupp[1,2], **Carl S. Miller**[1], **Matthew P. Reed**[1,4], **Nathaniel H. Madura**[1], **Nichole L. Ritchie**[1], **and Lawrence W. Schneider**[1,3]
[1]University of Michigan Transportation Research Institute (UMTRI)
[2]The University of Michigan, Department of Emergency Medicine
[3]The University Michigan, Department of Biomedical Engineering
[4] The University Michigan, Department of Industrial and Operations Engineering

United States
Paper 07-0345

ABSTRACT

Analyses were performed to quantify the conditions under which the knee is loaded in frontal motor-vehicle crashes and to thereby provide insight on the test conditions that should be used in future studies of the tolerance of the knee to loading of its anterior surface. These analyses estimated knee angle and the orientation of the femur relative to the knee bolster during bolster loading, the area of knee over which knee bolster contact loads are distributed, and knee loading rate. The postures of the lower extremities of 18 male and 18 female occupants relative to the knee bolster in three vehicles were used with a 2D kinematic model of the lower extremities to estimate occupant knee angle and the angle between the long axis of the femur and the plane of the knee bolster at initial knee contact and after 100 mm of bolster stroke. At knee contact, the average knee angle was 92˚ ± 13˚ (mean ± sd) and average bolster-to-femur angle was 67˚± 6˚. After 100 mm of bolster stroke knee angle was reduced to 75˚ ± 11˚ and bolster-to-femur angle was 65˚ ± 5˚. Bolster-to-knee contact areas produced by a single set of cadaver knees impacting four driver knee bolsters selected for their widely varying force-deflection characteristics resulted in forces being distributed over the majority of the anterior surface of the patella. Analysis of femur force histories in FMVSS 208 and NCAP tests indicated that median femur loading rate was approximately 250 N /ms and 90% of femur loading rates were below 1 kN/ms. These values are only rough estimates of knee loading rates, since contributions of axial and shear forces transmitted through the knee to axial femur force are not quantified in FMVSS 208 and NCAP tests.

INTRODUCTION

A research program is underway at the University of Michigan Transportation Research Institute to develop new injury criteria and injury assessment reference values (IARVs) for the knee-thigh-hip (KTH) complex. A recent focus of this effort is to better understand the injury tolerance of the anterior surface of the flexed knee to knee-bolster loading.

Studies in the biomechanical literature have demonstrated that the stiffness of the surface loading of the knee can have a large effect on knee fracture tolerance. However, none of stiffnessess of the surfaces used to load the knees in these studies have been related to the stiffness of production knee bolsters. Atkinson et al. (1997) analyzed knee-thigh-hip injury patterns produced by knee impacts from tests in which the flexed knees of seated cadavers were dynamically loaded with flat-faced rigid and padded impactors (Patrick et al. 1967, Powell et al. 1975, Melvin et al. 1975, and Stalnaker and Viano 1980) and found that rigid impacts are associated with a greater proportion of knee fractures than padded impacts.

Atkinson et al. also reported on a series of biomechanical tests that further demonstrates that the compliance of the surface impacting the knee can affect knee tolerance. In these tests, pairs of knees from unembalmed cadavers were dynamically loaded in a 90˚-flexed posture, such that one knee was impacted with a rigid surface and the contralateral knee was impacted with an energy-absorbing surface. Tests that used a rigid impactor applied a focal load to the knee and produced fractures of the patella or of the patella and femoral condyles at an average force of 5 kN. In contrast, tests that used an energy-absorbing impactor distributed impact forces over the entire anterior surface of the patella and did not produce any injuries, even though peak knee impact forces were approximately 20% higher than those from the corresponding rigid impacts. Despite the strong association between knee tolerance and the manner in which force was distributed over the anterior knee surface, the stiffnesses and knee contact areas produced by the energy-absorbing knee impactors were not compared to those of the surfaces being loaded by driver knees in frontal crashes.

Studies in the biomechanical literature have also hypothesized that knee angle affects knee fracture pattern because changes in knee angle alter the position of the patella on the femoral condyles (Haut

1989, Atkinson et al. 1997). A more flexed knee results in a patella that is located between the femoral condyles, which is thought to be associated with a greater likelihood of split condylar fractures and the surpacondylar fractures that result from split condylar fractures. Conversely, a more extended knee is associated with a patellar position that is above the femoral condyles and is therefore thought to be less likely to split the femoral condyles and more likely to result in fracture of the patella. If these hypotheses are correct, and changes in knee angle are associated with changes in injury pattern, then changes in knee angle may also be associated with differences in knee tolerance.

Another limitation of knee tolerance data in the biomechanical literature is that all of these data were collected in tests in which the knee is loaded by flat surfaces that are perpendicular to the long axis of the femur. In real-world frontal crashes, it is likely that variability in occupant posture, coupled with the initial angle of the knee bolster, results in knee loading that is not perpendicular to the long axis of the femur. If the knee bolster is angled relative to the long axis of the femur, the patella will be forced downward relative to the femoral condyles during knee bolster loading, which may affect knee fracture pattern and knee tolerance.

The current study was performed to provide a foundation for future knee tolerance research by defining the ranges over which test parameters should be varied. Data on occupant posture, position, and vehicle interior geometry were analyzed to estimate the ranges of knee angles and the orientation of the knee bolster relative to the long axis of the femur during bolster loading in frontal crashes. Cadaver knees were impacted by knee bolsters from production vehicles to estimate how load is distributed over the anterior surface of the knee. Loading rates and peak femur forces from FMVSS 208 and NCAP tests were analyzed to provide rough estimates of knee loading rate and peak force applied to the knee in severe full-frontal crashes.

METHODS

Knee and Knee-Bolster-to-Femur Angles

Variations in knee angle and the angle of the knee bolster relative to the long axis of the femur during frontal crashes were estimated using occupant anthropometry, posture, position, and vehicle interior package geometry collected as part of an unpublished previous study at UMTRI in which the seated postures and positions of 18 male and 18 female subjects were recording following normal driving in three vehicles. These subjects were selected using a stature-based criterion so that tall and short drivers were oversampled relative to the US population, thus allowing a better estimate of the effects of stature on driver posture and position. The three vehicles used in this study were selected because they varied in seat height (H30) and included a midsize sedan (2002 Pontiac Grand Am), a large sedan (2000 Ford Taurus), and a minivan (2001 Dodge Caravan). Figure 2 illustrates the relevant driver lower-extremity posture data that were collected. These data include the locations of the left lateral malleolus, lateral femoral condyle, greater trochanter, and suprapatellar landmark.

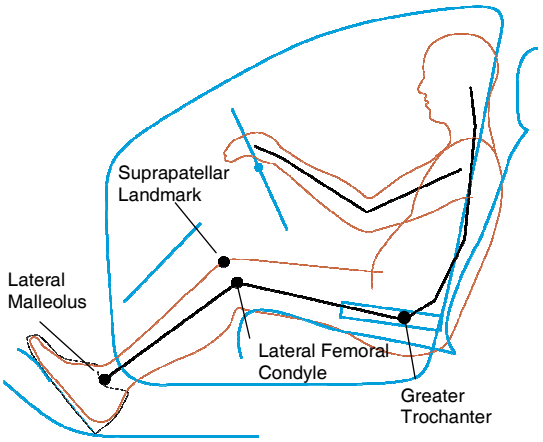

Figure 2. Skeletal landmarks collected in UMTRI studies to define the posture of the driver's lower extermities.

A simple 2D model of the right side of the lower extremities was generated for each occupant in each vehicle package using the points illustrated in Figure 2. This model was used to predict knee angle and bolster-to-femur angle at the time of knee bolster contact by translating the hip forward horizontally while constraining the leg to rotate about an ankle joint (i.e., the lateral malleolus) that was fixed with respect to the vehicle interior until the suprapatellar landmark intersected the plane of the knee bolster. Figure 3 illustrates this posture and defines knee angle and bolster-to-femur angle. These angles were also calculated after 100 mm of knee bolster stroke, which was simulated by moving the knee bolster away from the occupant's knees by 100 mm and repeating the procedure used to determine knee and bolster-to-femur angles at knee bolster contact.

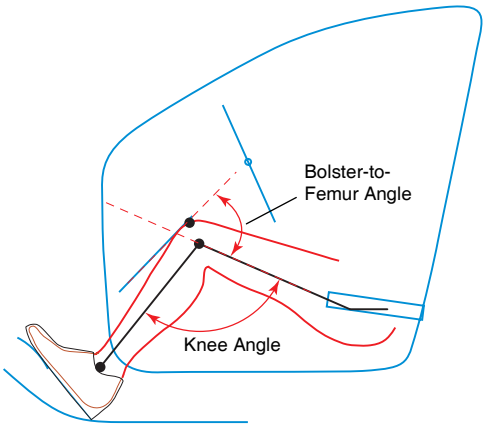

Figure 3. Two-dimensional linkage model of occupant's knee, thigh, leg, and ankle at the time of knee bolster contact illustrating knee and knee-bolster-to-femur angles.

Because the subjects in the driver posture study included a greater proportion of tall men and short women than would be expected in a typical driver population, it was necessary to reweight the predictions of the kinematic model to appropriately estimate the tail percentiles of the expected distributions of model predicted posture variables. The procedure used to do this is similar to the method reported by Flannagan et al. (1998) for analyzing data from stratified samples. In brief, linear regression functions are computed to predict the relationship between stature and posture variables (i.e., knee angle and bolster-to-femur angle) for each gender and each vehicle. If a meaningful relationship between a posture variable and stature exists, the distributions of knee angle and bolster-to-femur angles can be estimated by convolving the single-gender stature distribution by the linear regression model and adding the normally distributed residual variance from the regression. Percentiles of bolster-to-femur angle for each vehicle were calculated by combining the two single-gender normal distributions. If there is not a relationship between a posture variable and stature, tail percentiles can be estimated from the model-predicted distributions of the posture variable.

Knee contact area

Knee specimens from a single midsize male unembalmed cadaver were obtained by sectioning the lower extremities of a single midsize male cadaver slightly distal of the midshaft of the femur. These specimens were impacted by driver-side instrument panel/knee bolster (IP/KB) assemblies from four production vehicles to collect data on the area of the knee surface loaded by the knee bolster in a frontal crash. Instrument panel/knee bolster assemblies were obtained from the vehicles listed in Table 1. These vehicles were selected because knee bolster force-deflection data from an earlier series of IP/KB tests (available at www-nrd.nhtsa.dot.gov, test numbers 8278-8291) indicate that knee bolsters from these vehicles should have a wide range of force-deflection characteristics and are therefore likely to produce a wide range of knee contact areas. Also, loading rates and peak femur forces from FMVSS 208 tests of the vehicles listed in Table 1 span over 90% of the variance in peak femur force and loading in FMVSS 208 testing, which further suggests that knee contact areas and force-deflection characteristics of these knee bolsters should vary widely.

Table 1. Vehicle Knee Bolsters Tested

Test ID	Make	Model
NKB0612D	Ford	1998 Explorer
NKB0613D	Ford	2000 Focus
NKB0614D	Ford	2003 Escape
NKB0615D	Ford	2001 Taurus

Figure 4 illustrates the test apparatus and Figure 5 provides more detail on the knee mounting hardware and instrumentation. Prior to testing, each IP was cut approximately in half. The driver side of each IP was then rigidly attached to a linearly translating sled using rigid brackets that were connected to structures supporting the IP (most commonly the cross-car beam) and bolted to the sled. Mounting the IP in this manner ensured that the knee bolster and its supporting hardware were intact and thereby ensured that the structural characteristics of the knee bolster were not affected by removal of the passenger side of the IP.

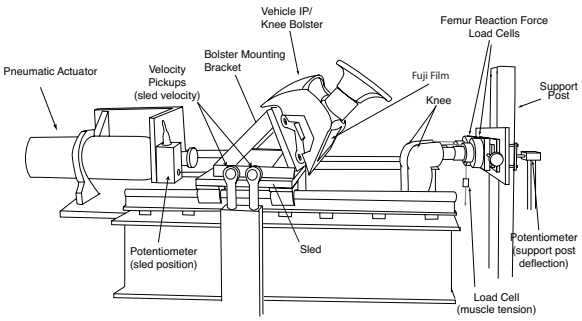

Figure 4. Side view of test apparatus.

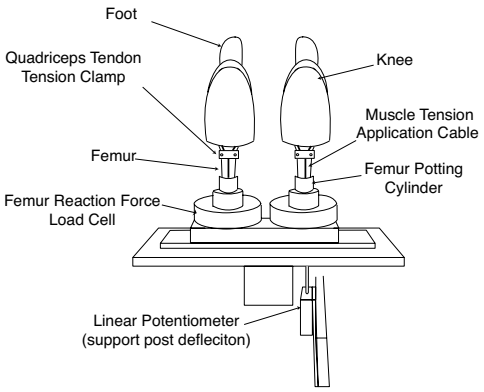

Figure 5. Top view of knee-mounting scheme.

The knee specimens used in these tests were obtained by sectioning the femurs of a single midsize male cadaver at midshaft and potting the truncated ends with room-temperature-curing epoxy. As shown in Figure 5, the potted ends of the femurs were rigidly secured to load cells that were attached to a support post. Both femurs were mounted so that the anterior surfaces of the knees were the same distance forward of the support post. The feet were supported from below by a platform and secured by clamping the ankles to a support positioned immediately behind each heel. For each test, approximately 600 N of tension was applied to each quadriceps tendon along its typical line of action by specialized clamps that were connected to a pneumatic cylinder by means of steel cables that were routed through holes drilled through the potting compound.

All tests were performed with a knee angle of approximately 90˚ and with the knee bolster oriented to produce a bolster-to-femur angle of approximately 65˚, which are the approximate average values for these quantities based on the simulations described in the previous section. For each test, the lateral space between the knees was set to achieve the knee-bolster contact locations observed in FMVSS 208 tests of vehicles that were similar to those from which the knee bolster being tested was obtained.

Contact area was measured by layers of medium (10-50 MPa) and low (2.5-10 MPa) pressure-sensitive Fuji prescale film that were attached to the knee bolster surface. Due to the irregular shapes of the knee bolsters, sheets of prescale film were cut and shaped to follow the contour of the bolster. This also limited the artifacts caused by creases in the film.

To conduct a test, the knee bolster was pneumatically accelerated to a velocity of approximately 1.5 m/s prior to contact with the stationary knee/leg specimens. This impact velocity and the ~300 kg platform mass were selected to produce an impact energy of 350 J, which was found to produce femur loading rates and peak forces similar to those measured in FMVSS 207 tests of the vehicles listed in Table 1 when KB/IP assemblies from these vehicles were loaded by Hybrid III knees in an earlier series of tests (available at www-nrd.nhtsa.dot.gov, test numbers 8278-8291).

Force applied to each knee was measured by a six-axis load cell positioned behind the potted femur. The force-deflection characteristics of the knee bolster were measured using the average of the left and right femur force histories and the displacement of the platform following knee contact. Average knee-bolster stiffness was calculated by taking the slope of the loading portion of the force-deflection curve between the deflection at which force first exceeded 15% of its maximum value and the deflection at which force last exceeded 85% of peak force. Average knee-bolster loading rate was calculated from the loading portion of the average force history in a similar manner. Each knee bolster was only tested once and the knees of the test specimen were palpated between tests to ensure that gross knee fracture had not occurred.

FMVSS 208 and NCAP Analysis

Femur force histories from FMVSS 208 and NCAP tests conducted between 1998 and 2004 from the NHTSA vehicle database were analyzed to characterize peak femur force and loading rate. A total of 1548 femur force histories from driver and right-front-seat passenger ATDs in 387 frontal impacts were analyzed. Loading rates were calculated by taking the slope of the loading portion of the force histories from the time the force first exceeds 15% of its peak value to the time the force last exceeds 85% of its peak. Table 2 describes the deltaVs, test types, and belt use in these crashes. Eighty of the eighty-nine FMVSS 208 tests were performed using unbelted ATDs and either a 48-kph soft pulse sled test (60/89) or a 40-kph barrier impact (20/89). The remaining nine tests were performed using belted occupants in the same test types. All 298 NCAP tests were performed using a 56-kph barrier impact with belted driver and right-front passenger ATDs.

Table 2. Characteristics of 1998-2004 FMVSS 208 and NCAP Frontal Impacts in the NHTSA Database

Test Category	Test Type	Nominal DeltaV (kph)	Belted/ Unbelted	# of Tests
FMVSS 208	Barrier	40	Unbelted	20
			Belted	1
		48	Unbelted	1
			Belted	6
	Sled	48	Unbelted	60
NCAP	Barrier	56	Belted	298

RESULTS

Knee and Knee-Bolster-to-Femur Angles

The average knee angles calculated for the 36 driver test subjects are listed in Table 3 for each of the three vehicles. Figures 6 and 7 show that occupant stature has no effect on knee angle at the time of bolster contact or after 100 mm of bolster stroke for all three vehicles. Because knee angle is not related to stature, it is not necessary to account for the effects of the over representation of tall men and short women in the subject population from which posture data were obtained.

Knee angle data were approximately normally distributed. Mean knee angle at contact was 92˚±13˚ (mean±sd) across vehicles, which is an average of 29˚ less than the starting knee angle. After 100 mm of simulated bolster stroke, knee angle was reduced by an average of 17˚ to a mean of 75˚±11˚, suggesting that most knee bolster loading occurs at knee angles that are less than 90˚. The 5th and 95th percentile knee angles are 67˚ and 116˚ at bolster contact and 54˚ and 96˚ after 100 mm of bolster stroke.

Table 4 lists the knee-bolster-to-femur angles predicted by the simulations. At the time of knee-to-knee-bolster contact, the mean angle between the femur and the knee bolster surface is approximately 65˚. This angle changed by an average of only 2˚ after 100 mm of simulated bolster stroke.

Figures 8 and 9 show a meaningful relationship between stature and bolster-to-femur angle at initial knee contact and after 100 mm of simulated bolster stroke, with short statured occupants having smaller bolster-to-femur angles and taller occupants having bolster-to-femur angles that were closer to 90˚. This trend probably occurred because short occupants have shorter legs and therefore start with a smaller bolster-to-femur angle.

After accounting for the effects of the sampling scheme used in the UMTRI study from which posture data were obtained, mean bolster-to-femur angle at knee contact was 65˚±5˚ and the 5th and 95th percentile bolster-to-femur angles were 56˚ and 74˚, respectively. After 100 mm of bolster stroke, bolster-to-femur angle did not change substantially. Mean bolster-to-femur angle was 67˚±6˚ and the 5th and 95th percentile bolster-to-femur angles after 100 mm of bolster stroke were 57˚ and 77˚, respectively.

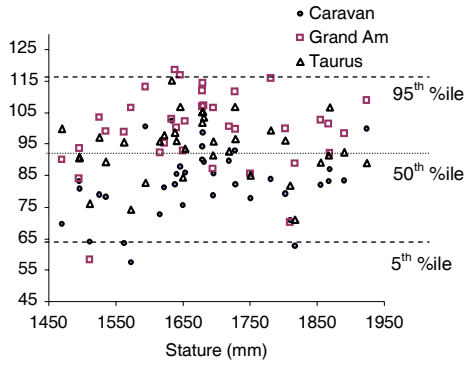

Figure 6. Knee angle at bolster contact versus occupant stature for the Caravan, Grand Am, and Taurus. Percentiles are from the combined data from all vehicles and occupants.

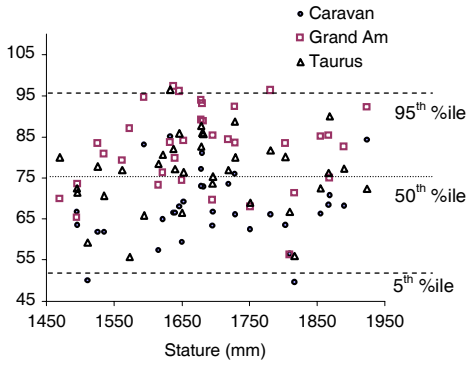

Figure 7. Knee angle after 100 mm of bolster stroke versus occupant stature for the Caravan, Grand Am, and Taurus. Percentiles are from the combined data from all vehicles and occupants.

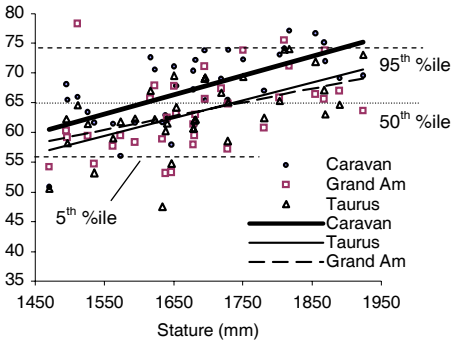

Figure 8. Bolster-to-femur angle at bolster contact to occupant stature for the Caravan, Grand Am and Taurus. Percentiles are from the combined data from all vehicles and occupants.

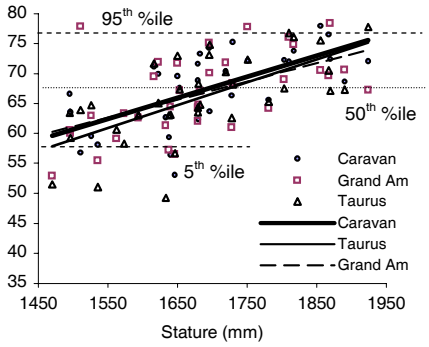

Figure 9. Bolster-to-femur angle after 100 mm of bolster stroke to occupant stature for the Caravan, Grand Am and Taurus. Percentiles are from the combined data from all vehicles and occupants.

Table 3. Mean Calculated Knee Angles

Vehicle	Initial Posture (degrees)	Bolster Contact (degrees)	100 mm of Bolster Stroke (degrees)	Change to Bolster Contact (degrees)	Change at 100 mm of Bolster Stroke (degrees)
Caravan	118	82	68	-36	-15
Grand Am	127	99	81	-27	-18
Taurus	119	94	76	-25	-18
All	121	92	75	-29	-17

Table 4. Mean Calculated Bolster-to-Femur Angles

Vehicle	Initial Posture (degrees)	Bolster Contact (degrees)	100 mm of Bolster Stroke (degrees)	Change to Bolster Contact (degrees)	Change at 100 mm of Bolster Stroke (degrees)
Caravan	63	67	67	4	0
Grand Am	57	63	67	6	3
Taurus	58	63	66	5	3
All	59	65	67	5	2

Knee Contact Area

Autopsy of the cadaver knees following the completion of all tests indicated that loading of the single pair of cadaver knees applied by all four of the knee bolsters did not produce any injuries. Table 5 summarizes results from each test. Peak force measured behind each knee ranged from 2.7 kN to 4.5 kN. Although both knees contacted the knee bolster at the same time in all four tests, peak forces applied to the left and right knees varied, suggesting that the force-deflection characteristics of the left and right sides of the knee bolster differ. The average knee penetration into the knee bolster varied from 79 mm to 94 mm. Knee bolster stiffness varied from 30 to 114 N/mm. In all tests, applied force peaked before maximum platform displacement, indicating bolster stiffness decreases after some amount of bolster deformation.

Figure 10 shows side-view high-speed video images of the left and right sides of the knee bolster at the times of knee contact and peak force for the Explorer, Focus, Escape, and Taurus knee bolsters. Figure 11 shows the contact areas measured by the low-pressure Fuji Film relative to the patella and femoral condyles from the single cadaver knee that was tested. These data provide insight on how the knee

bolsters deformed. The images from tests of the Explorer, Focus and Escape in Figure 10 show the bolster wrapping around the knee. The Fuji films from the corresponding tests show contact areas that are distributed over the entire surface of the patella. The images of the Taurus knee bolster shown in Figure 10 and the contact areas for the Taurus shown in Figure 11 (which only covers part of the patellar surface and one femoral condyle) indicate that the Taurus bolster did not fold around the knees, but instead the forward surface of the bolster displaced rearward as a unit.

Table 5. Cadaver Knee-to-Knee-Bolster Force and Displacement Results

Model	Peak Force, Left / Right (kN)	Penetration into Bolster (mm)	Loading Rate (N/ms)	Bolster Stiffness (N/mm)
Explorer	3.8/4.5	79	200	114
Focus	2.8/4.3	93	47	30
Escape	2.7/3.0	94	200	106
Taurus	3.6/4.2	91	53	38

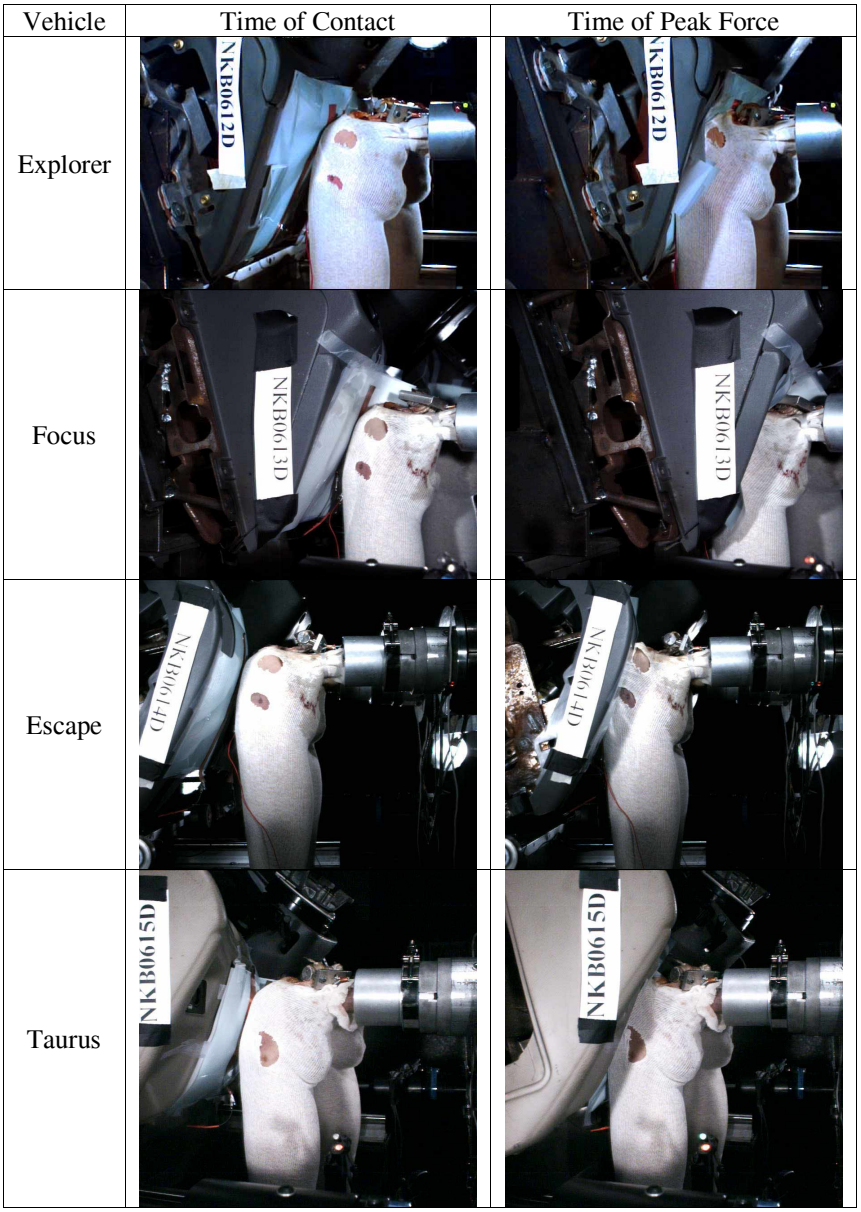

Figure 10. Images from side-view high-speed video showing deformation of KB/IP assemblies.

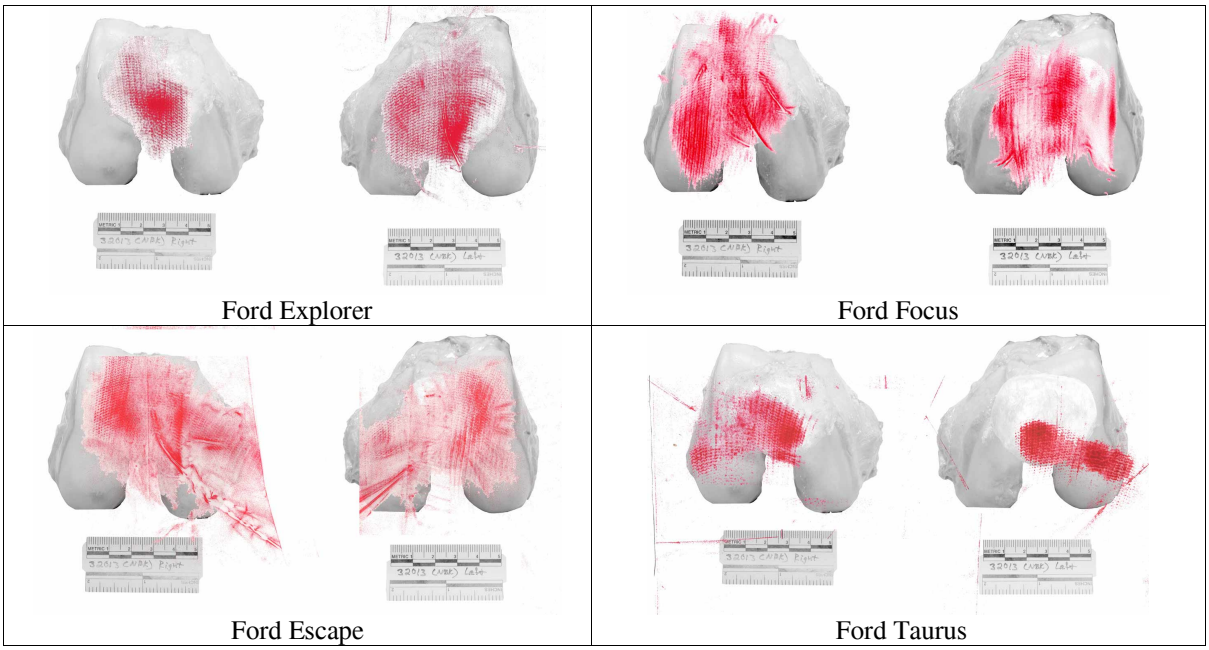

Figure 11. Contact areas recorded during tests of Explorer (upper left), Focus (upper right), Escape (lower left), and Taurus (lower right).

FMVSS 208 and NCAP Analysis

Figure 12 shows the combinations of peak compressive femur force and femur loading rate produced in NCAP and FMVSS 208 tests. Table 6 provides quantile values that describe the individual distributions of these parameters. The median peak force for NCAP tests is 3.6 kN and the median peak force for FMVSS 208 tests is 4.8 kN. The median loading rate for both FMVSS 208 and NCAP tests is approximately 250 N/ms and 90% of tests produced loading rates that were less than approximately 1 kN/ms. In general, NCAP tests produced a greater range of peak forces and loading rates than FMVSS 208 tests. This is expected since there are a greater number of NCAP tests and these tests involve a higher deltaV. In addition, these tests involve belted occupants who contact the knee bolster either earlier or later in the crash depending on the pre-impact knee-to-knee bolster spacing, belt restraint characteristics, and the crash pulse.

Although belt use and deltaV varied within the set of FMVSS 208 tests that was analyzed, changes in belt use and deltaV did not produce meaningful changes in loading rates or peak forces because differences between vehicles have a greater effect on these parameters than the differences between types of FMVSS 208 tests.

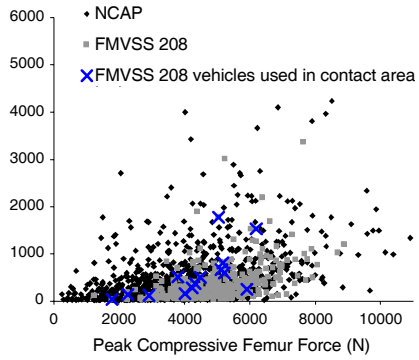

Figure 12. Combinations of peak force and loading rate from FMVSS 208 and NCAP frontal impacts conducted between 1998 and 2004.

Figure 12 also shows the peak forces and femur loading rates for FMVSS 208 tests in which the driver knee bolsters used in the knee contact area testing were loaded (i.e., knee bolsters from the Escape, Explorer, Focus, and Taurus). The ranges of peak force and femur loading rates produced in this subset of force histories were 1.7 kN to 6.2 kN and 40 N/ms to 1800 N/ms, respectively. As shown in Table 5, these ranges incorporate over 90% of the loading rates and peak forces produced in FMVSS 208 tests, suggesting that the knee bolsters used in the knee contact area tests provide a reasonable approximation of the range of knee bolsters in production vehicles.

Table 6. Peak Force and Loading Rate Quantiles for NCAP and FMVSS 208
Femur Force Histories from 1998-2004

	FMVSS 208 (n = 346)		NCAP (n = 1202)		FMVSS 208 and NCAP (n=1548)	
Quantile	Peak Force (N)	Loading Rate (N/ms)	Peak Force (N)	Loading Rate (N/ms)	Peak Force (N)	Loading Rate (N/ms)
100.0%	8897	3364	10910	5567	10910	5567
99.5%	8753	3121	9774	3897	9610	3636
97.5%	7642	1460	7727	2061	7639	1964
90.0%	6478	824	6152	1107	6277	1027
75.0%	5741	468	4856	571	5141	538
50.0%	4793	250	3618	246	3970	249
25.0%	4030	110	2395	92	2709	98
10.0%	3298	69	1416	44	1627	51
2.5%	2251	42	613	26	714	29
0.5%	1184	28	329	21	346	21
0.0%	1023	28	171	20	171	20

DISCUSSION

Three types of analyses were conducted to characterize the knee loading environment in frontal crashes. These include analyses of driver lower-extremity postures relative to knee bolsters during bolster loading, tests to characterize contact areas produced by production driver knee bolsters loading cadaver knees, and analysis of FMVSS 208 and NCAP data to characterize ranges of peak femur forces and loading rates.

Analyses to determine knee angle and bolster-to-femur angle at knee bolster contact and after 100 mm of knee bolster stroke were performed using a 2D kinematic model of the lower extremities that was generated using positions of skeletal surface landmarks relative to vehicle interior components measured from 36 drivers in three vehicles. Because the interior geometries of the entire vehicle population vary more than those of these three vehicles, and because variations in vehicle geometry will change preimpact knee-to-knee bolster spacing and occupant lower extremity posture, which in turn, affect knee angle and bolster-to-femur angle at knee contact, the knee angles and bolster-to-femur predicted by the 2D kinematic model should be considered conservative estimates of the ranges of these parameters for the driver/vehicle population.

In addition, in the simulations with the 2D kinematic model it was assumed that the position of the ankle remains fixed prior to bolster contact. This assumption may not be reasonable for knee-to-knee bolster loading in real crashes, where vehicle deceleration may cause the foot to move forward or toepan intrusion may cause the foot to move rearward, thereby making the knee angle either more or less acute.

Tests in which the knees of a single cadaver were loaded by four driver IP/knee bolster assemblies were performed to characterize the area of the anterior surface of the knee that is loaded by knee bolsters. These knee bolsters have widely variable force-deflection characteristics and because FMVSS 208 peak femur forces and femur loading rates further suggest that these results can likely be generalized to knee bolster loading in full-frontal crashes where the occupant's femurs are aligned with the 12 o'clock PDOF. These findings may not be applicable to angled or offset frontal crashes, or cases where occupants have large amounts of leg splay prior to bolster impact because these conditions result in smaller knee-to-knee bolster contact areas (Meyer and Haut, 2004).

The real-world applicability of the data reported in this study is predicated on the assumption that the knees contact the knee bolster in frontal crashes. While this assumption is valid for NCAP and FMVSS 208 crashes with ATDs, and therefore is valid for the using in biomechanical testing aimed at developing injury criteria and IARVs, it may not be valid for crashes angled and offset frontal crashes involving human occupants who will sit differently than ATDs. Because of these differences in occupant posture and crash dynamics, the knees of human occupants may contact surfaces other than the knee bolster (e.g., the steering column). If these surfaces have different geometries and force-deflection

characteristics than knee bolsters, then the contact areas, knee loading rates, knee angles, and bolster-to-femur angles reported in this study may not be applicable to knee-thigh-hip injury causation scenarios in these crash types. To determine the validity of the assumption that most knee-thigh-hip injuries in frontal crashes are caused by knee bolster contact, knee contacts associated with knee-thigh-hip injury in CIREN were analyzed. The results of this analysis are described in detail in the appendix. In brief, the 80% of the KTH injuries sustained by drivers and 64% of the KTH injuries sustained by right-front passengers in frontal crashes were associated with knee bolster contact. This finding indicates that it is appropriate to measure knee tolerance under knee-bolster-like loading conditions.

The analyses of FMVSS 208 and NCAP ATD femur force histories that were performed in this study only provide rough estimates of knee loading rate and peak force applied to the knee in frontal crashes. This is because it is not possible to accurately determine the force applied to the knee (or knee loading rate) in a frontal crash without knowledge of the compressive force on the upper tibia and the shear force at the knee, neither of which are currently measured in FMVSS 208 and NCAP tests. In addition, the acceleration of the distal femur is not measured, making it difficult to account for inertial effects on the decrease in force between the knee and the femur load cell.

The peak femur forces and loading rates measured at by the Hybrid III femur load cell are also difficult to relate to the femur and knee loading rates and peak forces that would be produced by a midsize male human loading the knee bolster. Specifically, the Hybrid III knee-thigh-hip complex is stiffer and has more tightly coupled mass than the cadaver, and presumably the human, knee-thigh-hip complex, Hybrid III knee impact forces and knee and loading rates are likely to be higher than those applied to the human knee (Rupp et al. 2005).

Despite the difficulties in estimating knee loading rate and peak force applied to the human knee using Hybrid III femur load cell data, the knee loading conditions produced in FMVSS 208 and NCAP can be reproduced experimentally, if the contribution of force transmitted through the tibia to femur loading rate is assumed to be negligible. Specifically, an impactor could be designed that produces Hybrid III femur loading rates that are within the range of those produced in FMVSS 208 and NCAP tests.

This study demonstrates that knee bolster loading is distributed over most of the anterior surface of the patella, suggesting that the low fracture forces reported in the literature for rigid knee impacts do not need to be considered when evaluating vehicle knee bolster performance. The findings from this study also indicate that knee angle can vary substantially at the time of knee bolster contact and that knee angle decreases as the knee strokes the knee bolster. If knee angle affects knee injury tolerance, then existing knee tolerance data that have been collected using a ~90˚ flexed knee do not consider an important factor that affects knee tolerance in frontal crashes.

The findings in this study provide estimates of the ranges of parameters that should be used in future studies of the tolerance of the flexed knee to loading of its anterior surface by a knee-bolster-like surface. These ranges are listed in Table 7. If a worst-case scenario for knee tolerance is simulated, the compliance of the surface loading the knee should be set so that applied forces are distributed over most of the patella. Knee loading rate should be tuned to produce a knee loading condition that results in a loading rate at the Hybrid III femur load cell that is less than approximately 1 kN/ms. To simulate most of the variance in knee angles at bolster contact, knee posture should be varied by approximately ±20˚ from a value between approximately 90˚ and 75˚. The former value should be chosen if knee angle at contact is simulated, the latter if knee angle after the bolster is fully compressed is simulated. The surface loading the knee in these studies should be angled approximately 65˚±9˚ from the long axis of the femur to simulate most of the variance in the occupant and vehicle population.

Table 7. Ranges of Test Parameters for Future Studies of Knee Tolerance

Parameter	Target Range
Knee contact area	Distributed over the majority of the anterior surface of the patella
Knee angle	110˚ to 70˚, if posture at contact is simulated 95˚ to 55˚ if posture after 100 mm of stroke is simulated
Bolster-to-femur angle	65˚±9˚
Knee loading rate	< ~1kN/ms

CONCLUSIONS

These analyses suggest that:

- Ninety percent of the knee angles at the time of knee bolster contact for the driving population are between 67˚ and 116˚. After 100 mm of bolster stroke, ninety percent of knee angles are between 54˚ and 96˚.
- The average orientation of the long axis of the femur relative to the plane of the knee bolster is approximately 65˚ and ninety percent of bolster-to-femur angles lie between 56˚ and 74˚. This angle does not meaningfully change after 100 mm of knee bolster stroke.
- Ninety percent of knee-to-knee-bolster loading in FMVSS 208 and NCAP tests produces femur loading rates less than 1 kN/ms.
- Bolster-to-knee loading is distributed over most of the anterior surface of the patella and may be distributed over the entire patella and part of the femoral condyles.

These ranges of knee angle, bolster-to-femur angle, femur loading rate, and knee contact area provide bounds on the parameters that should be used, or produced, in future studies of knee tolerance to loading of the anterior surface of the flexed knee.

ACKNOWLEDGEMENTS

The research described in this paper was sponsored by the National Highway Traffic Safety Administration, U.S. Department of Transportation under contract # DTNH22-05-H-01020. The authors recognize Thomas Jeffreys for his assistance in specimen preparation and testing. The authors would also like to acknowledge the contributions of Charles Bradley, Brian Eby, Stewart Simonett, and James Whitley who assisted in the fabrication of the test apparatus. The assistance of Kathy Klinich in the review of this manuscript is gratefully acknowledged. The advice and guidance provided by Shashi Kuppa is acknowledged and appreciated. The assistance in gathering FMVSS 208 and NCAP femur force histories provided by Felicia McKoy of OnPoint is also gratefully acknowledged.

REFERENCES

Atkinson, P.J., Garcia, J.J., Altiero, N.J., and Haut, R.C. (1997). The influence of impact interface on human knee injury: Implications for instrument panel design and the lower extremity injury criterion. Proceedings of the 41st Stapp Car Crash Conference, Paper No. 973327, pp. 167-180. Society of Automotive Engineers, Warrendale, PA.

Haut, R.H. (1989). Contact pressures in the patellofemoral joint during impact loading on the human flexed knee. Journal of Biomechanics 7:272-280.

Flannagan, C., Manary, M.A., Schneider, L.W., and Reed, M.P. (1998). An improved seating accommodation model with application to different user populations. Journal of Passenger Cars 107:1189-1197.

Melvin, J.W., Stalnaker, R.L., Alem, N.M., Benson, J.B., and Mohan, D. (1975). Impact response and tolerance of the lower extremities. Proceedings of the Nineteenth Stapp Car Crash Conference. Paper No. 751159, 543-559. Society of Automotive Engineers, Warrendale PA.

Melvin, J.W. and Stalnaker, R.L. (1976). Tolerance and response of the knee-femur-pelvis complex to axial impact. Report No. UM-HSRI-76-33. University of Michigan, Highway Safety Research Institute, Ann Arbor, MI.

Meyer, E.A. and Haut, R.C. (2003). The effect of impact angle on knee tolerance to rigid impacts. Stapp Car Crash Journal 47:1-19.

Partick, L.M., Kroell, C.K., and Mertz, H.M. (1966). Forces on the human body in simulated crashes. Proceedings of the Ninth Stapp Car Crash Conference, pp. 237-260. University of Minnesota.

Powell, W.R., Ojala, S.J., Advani S.H., and Martin, R.B. (1975). Cadaver femur responses to longitudinal impacts. Proceedings of the Nineteenth Stapp Car Crash Conference, Paper No. 751160, 561-579. Society of Automotive Engineers, Warrendale PA.

Rupp, J.D., Reed, M.P., Madura, N.H., Kuppa, S., and Schneider L.W. (2003b) Comparison of knee/femur force-deflection response of the Thor, Hybrid III, and human cadaver to dynamic frontal-impact knee loading. Proceedings of the 18th International Conference in the Enhanced Safety of Vehicles. National Highway Traffic Safety Administration, Washington DC.

Stalnaker, R.L., Nusholtz, G.S., and Melvin J.W. (1977). Femur impact study. Final Report No. UM-HSRI-77-25. University of Michigan, Highway Safety Research Institute: Ann Arbor.

APPENDIX
KNEE CONTACTS IN CIREN

The CIREN database (1995-2006) was analyzed to identify the vehicle interior components that driver and passenger knees contact in frontal crashes that result in knee, thigh, or hip injury. In this analysis, only frontal crashes with PDOF between 10 o'clock and 2 o'clock were considered. Knee contacts in narrow frontal impacts with corner involvement (FLEE, FREE CDC codes) were excluded from the analysis, since the KTH injuries produced in narrow frontal impacts are often caused by the intruding door loading the thigh and hip, and not by knee contact. In addition, only knee contacts that were assigned a confidence level of certain or probable were used in the analysis.

Figure A1 shows the results of this analysis. Injuries that were associated with contact with the glove box were combined with those coded as the right knee bolster, since the glove box and right knee bolster are equivalent components. In addition, contacts coded "left IP and below" and "right IP and below" were combined with the left and right knee bolster codes, respectively, since the lower IP is typically designed to deform like the knee bolster. Eighty percent of KTH injuries experienced by the driver were attributed to knee bolster contact. A similar trend was observed for KTH injuries to passengers, where 64% of injuries were from knee bolster contacts. However, a greater proportion of passenger KTH injuries were associated with contacts to the center IP and below and the right door, armrest, and door hardware.

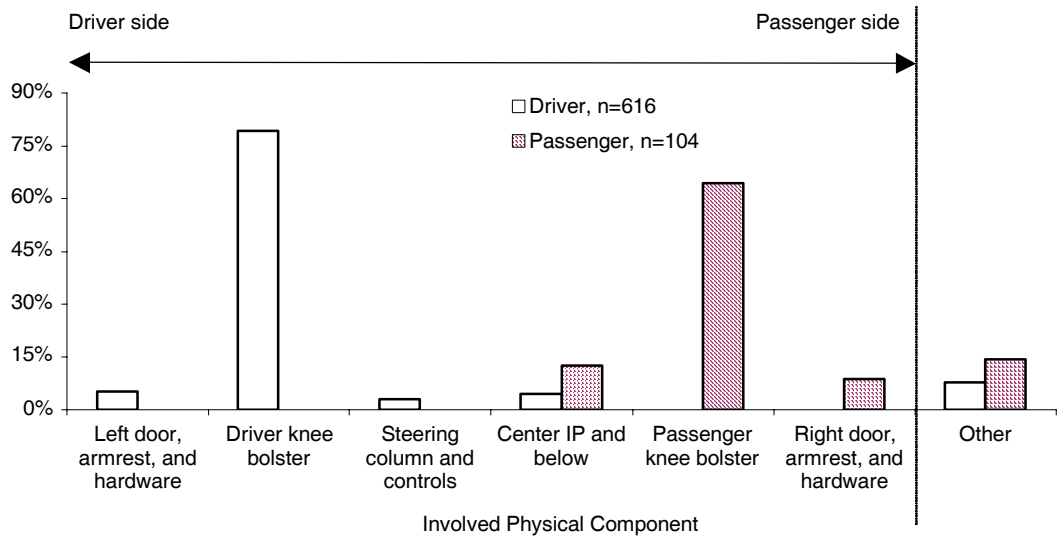

Figure A1. Proportion of driver and passenger AIS 2+ knee-thigh-hip injuries versus involved physical component contacted by the knee in frontal crashes in CIREN (1997-2006).